Pinning in proton-irradiated and annealed $YBa_2Cu_3O_{7-x}$ single crystals

M. L. Griffith and J. W. Halloran
Department of Materials Science and Engineering, The University of Michigan, Ann Arbor, Michigan 48109-2136
(Received 29 May 1992; revised manuscript received 10 August 1992)

Pinning in flux-grown $YBa_2Cu_3O_{7-x}$ single crystals is characterized with superconducting-quantum-interference-device magnetometry at 10 and 77 K. A wide variety of magnetic hysteresis behaviors are observed in crystals with different growth and oxygen annealing treatments, indicative of variable native pinning populations. These will be discussed in terms of the pinning forces (F_p) for the native pins. Irradiation at a dose of $10^{16}/cm^2$ with 3.4-MeV protons was used to increase the population of pinning defects. Changes in the flux-pinning parameters after postirradiation thermal anneals are used to determine the thermal stability of the defects responsible for the enhanced pinning. Isochronal anneals, $t=10$ min, were able to achieve total recovery to the preirradiated state by 600 °C. This annealing experiment revealed two stages of recovery for the enhanced pinning at 100 and 470 °C, respectively. By calculating theoretical Frenkel pair recovery curves, we found that oxygen point defects recombine between 100 and 200 °C, copper between 450 and 600 °C, and barium between 800 and 900 °C. The slowly diffusing yttrium was not considered. Since the annealing range of point defects is coincident with the experimental results, we conclude that oxygen and copper point defects are responsible for the excess pinning. Isothermal anneals, $T=450$ °C, verified that two species enhance the pinning properties which correlated to the O and Cu point defect model.

I. INTRODUCTION

The critical current density J_c of high-temperature superconductors (HTSC's) can be enhanced by irradiation so as to produce a high density of vortex-pinning defects. With irradiation of the $YBa_2Cu_3O_{7-x}$ (YBCO) superconductors by neutrons and ions, there has been much success in the enhancement of the critical properties.[1] However, the specific defects responsible for enhancing J_c have not been unambiguously identified and correlated to a plausible model for the amount of enhancement that is obtained.[2]

Through extensive irradiation studies,[3] researchers have found the critical dose, for a given energy and ion, to get the optimum enhancement in the superconducting properties (J_c,F_p) for which there is little or no change in the critical temperature T_c. With 3.4-MeV protons, the critical dose is in the range $1–2\times10^{16}$ ion/cm^2. This dose allows for the enhancement of J_c and F_p without degrading the critical temperature T_c.

By performing thermal annealing experiments on weak and strong native (as-grown) pinning YBCO single crystals that have been subsequently irradiated, we hope to determine how the excess pinning sites of the irradiated crystals recover during post-irradiation anneals. From the recovery temperatures, we can infer the nature of the defects responsible for excess pinning.

II. EXPERIMENTAL PROCEDURE

For the study of radiation-induced flux-pinning sites, YBCO single crystals were used. The specimens were obtained from T.A. Vanderah and were grown by a self-decanting flux technique.[4] The dimensions and critical temperatures of the four samples are given in Table I (part A). A Quantum Design superconducting-quantum-interference-device (SQUID) magnetometer was used, with the magnetic field parallel to the c axis, to characterize (zero-field cool) the samples at temperatures of 10 and 77 K for the full range of magnetic field (±5.5 T). From the magnetization data, a simple Bean model can transform the data into the critical-current density J_c and flux-pinning force F_p:

$$J_c=\frac{20(M_{\max}-M_{\min})}{L_1(1-L_1/3L_2)} ,$$

where $L_1<L_2$, and

$$F_p=J_cB .$$

The values for the critical-current density and flux-pinning force at 1 T for the native, as-grown crystals are summarized in Table I (part B).

Irradiation with 3.4-MeV protons was done at the Michigan Ion Beam Laboratory using the Tandem accelerator with a H^+ source. The irradiation was done at an angle of 7° with respect to the c axis to eliminate channeling effects. A dose of 1×10^{16} ions/cm^2 was chosen for the maximum effect on the flux-pinning properties. A pressure of 10^{-8} Torr was maintained for the reliability of the beam energy and to minimize contamination. The irradiation was done at room temperature, which was monitored by a thermocouple mounted to the sample holder, and heating effects during irradiation were reduced by using a low beam current of 340 nA. To produce the most flux-pinning sites vs depth, the samples were irradiated on both sides. The spatial distribution of the radiation will be discussed in Sec. III.

For the annealing study, the samples were heated in a small box furnace in air. To maintain the annealing tem-

TABLE I. Part A: Dimensions and critical temperatures of crystals. Part B: Flux pinning force at 10 and 77 K (1 T) for virgin and irradiated states.

A

Batch	Sample	L_2 (mm)	L_1 (mm)	t (μm)	T_c (K)
1	1	1.84	1.49	236.2	93.3
	2	2.28	1.30	99.1	93.3
2	3	1.29	0.89	208.3	92.7
	4	1.24	0.67	127.0	92.7

B

Virgin state

	$T=77$ K		$T=10$ K	
Sample	J_c (kA/cm^2)	F_p (GN/m^3)	J_c (MA/cm^2)	F_p (GN/m^3)
1	7.04	0.07	0.11	1.16
2	19.14	0.19	1.56	15.64
3	11.42	0.11	0.55	5.46
4	0.87	0.01	0.23	2.29

Irradiated state

	$T=77$ K		$T=10$ K	
Sample	J_c (kA/cm^2)	F_p (GN/m^3)	J_c (MA/cm^2)	F_p (GN/m^3)
1	70.46	0.71	1.05	10.50
2	127.45	1.27	4.26	42.63
3	15.44	0.15	1.64	16.38
4	0.53	0.01	0.87	8.67

perature during loading of the sample, a large thermal reservoir was placed inside the furnace with a thermocouple attached to it. The samples were very small, and so they reached thermal equilibrium within seconds when they were loaded or quenched. Between each anneal the samples were recharacterized in the magnetometer.

Two types of annealing experiments were done to reveal the thermal recovery range for the excess pinning and to determine or infer the defects responsible for enhancing the superconducting properties. An isochronal anneal was done to determine the thermal stability of the radiation-induced pinning sites. The temperature range of the annealing was 100–600 °C, in 50 °C increments. The time chosen for each temperature was 10 min. An isothermal anneal at 450 °C was done to examine the time dependence of the flux-pinning recovery process. Time increments of 10 min were used for a maximum of 50 min. The choices of temperatures for both anneals will become apparent in Sec. III.

III. RESULTS

A. Spatial distribution of radiation damage

In YBCO, 3.4-MeV protons have a range of 60 μm as calculated by the Monte Carlo program TRIM.[5] Figure 1 shows the results of the calculations for number of proton-collision events per ion (oxygen shown) vs depth. For depths up to 45 μm, the damage rate is roughly constant at 10^{-5} collisions/Å. This corresponds to a Frenkel-pair concentration of 545 ppm ($\sim 10^{18}$/cm^3) for oxygen. Similar curves and calculations exist for the other ions (Y,Ba,Cu) and their displacement concentrations are summarized in Table II. At the end of the range region in the damage profile, the defect concentration increases dramatically; for oxygen at 60 μm, the pair concentration is 22 530 ppm ($\sim 10^{20}$). With this many defects, it is likely that the end-of-range region is nonsuperconducting.[3] We call this the dead zone and expect it to be around 10–15 μm thick. Beneath this dead zone is an unirradiated region with virgin pinning effects. Figure 2 illustrates the regions that would exist in a thick single crystal.

Three out of four samples are thicker than the expect-

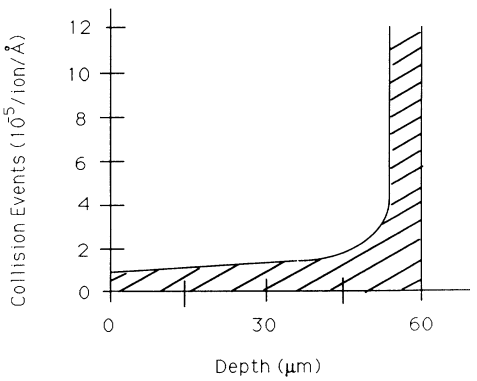

FIG. 1. Collision events for protons in the YBCO material: the damage rate concentration vs depth of oxygen irradiated with 3.4-MeV protons.

TABLE II. TRIM calculated displacements per atom in ppm for 3.4-MeV proton irradiation of YBCO.

Species	Frenkel pairs (ppm)
O	545
Cu	253
Ba	203
Y	153

TABLE III. Percentages of effect: nominal irradiation, dead zone, and unirradiated regions; and percent difference between the apparent J_c and the irradiated J_c (where the zones are taken into account).

Sample	Irradiated	Dead	Virgin	Percent difference
1	37.5	12.5	50.0	14.1
2	80.0	20.0	0	1.0
3	43.0	14.0	43.0	23.7
4	70.0	23.0	7.0	0.7

ed range (120 μm for both sides irradiated), and therefore three regions of spatial pinning exist. Table III lists the percentages of the regions for all four samples and shows that the effective irradiated zone varies between 37.5% and 80%. We report the "apparent" post-irradiation J_c from a simple Bean model, using the actual sample thickness. This overestimates the actual J_c in the samples by 0.7–23.7 %. The percent differences are listed in Table III for each sample. These were derived from a Bean model for the inhomogeneous sample, taking into account the actual dimensions of the irradiated, dead, and virgin zones.[6]

B. 10-K data

1. Virgin vs irradiated

For the virgin (preirradiated) YBCO single crystals, there exist different degrees of native pinning for the samples grown from the same batch. The samples range from weak to strong pinning as illustrated in Table I (part B).

In Fig. 3 it is shown for sample 4 (a weak native pinner) that the superconducting properties are enhanced by the proton irradiation. Up to 2 T, there is a fourfold increase in the magnetization which results in the same increase for J_c and F_p. Table I (part B), summarizes the results for all samples. There is an increase in the properties for all fields, but we will only present the data at 1 T.

2. Annealing experiments

Figure 4 presents the 1-T, 10-K isochronal recovery results for a strong-pinning sample (S2) and a weak-pinning sample (S1). These data are presented as the pinning force normalized by the pinning force for the virgin samples. All of the radiation-induced pinning has been annealed out by 600 °C. The enhanced pinning remains relatively constant (small amount of recovery) up to 450 °C, and then recovery to the virgin state proceeds abruptly for the weak-pinning sample at some temperature between 450 and 500 °C. The strong-pinning sample shows a drop in pinning force at 100 °C, followed by gradual recovery to the virgin state between the temperatures of 450 and 600 °C. It must be noted that the critical temperature T_c does not change after irradiation or after the annealing is complete.

The isothermal anneals were done at 450 °C since the results of the isochronal anneal revealed that 450 °C is the starting edge of the thermal recovery curve. The time increment of 10 min remained the same. From Fig. 5 it is indicated that there are two stages of recovery as illustrated by the change in slope after the 20-min anneal. Both samples in the first 10 min achieve, roughly, 50% recovery at 450 °C. The strong-pinning sample shows little change in F_p between 10 and 50 min, whereas the weak-pinning sample shows a gradual recovery with time. Neither crystal achieves full recovery to the virgin state after 50 min.

C. 77-K data

1. Virgin vs irradiated

As was shown with the 10-K data, proton irradiation improves the superconducting properties for the crystals at 77 K (Fig. 6 and Table I.B). The added defects show a more enhanced effect on the pinning properties at 77 K

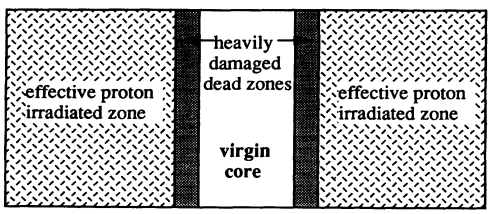

FIG. 2. Spatial irradiation regions in a single crystal of YBCO which is not proton transparent in thickness.

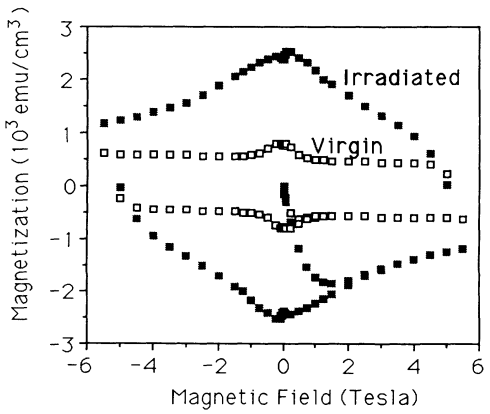

FIG. 3. Magnetic hysteresis loops for sample 4, a weak native pinner, before and after irradiation, characterized at 10 K.

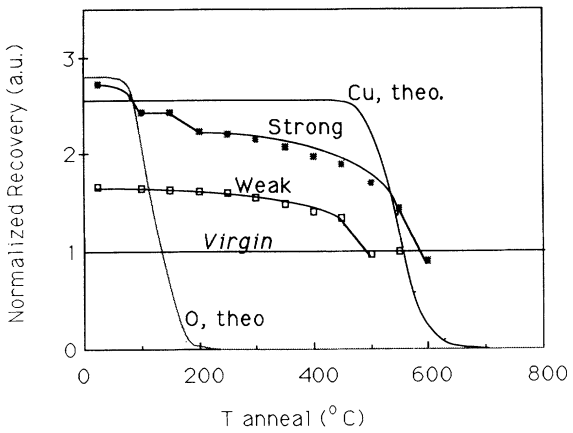

FIG. 4. Isochronal recovery at 10 K: experimental normalized flux-pinning force (to the virgin state) vs annealing temperature for strong (S2) and weak (S1) native pinning crystals with superimposed theoretical annealing curves for Cu and O point defects.

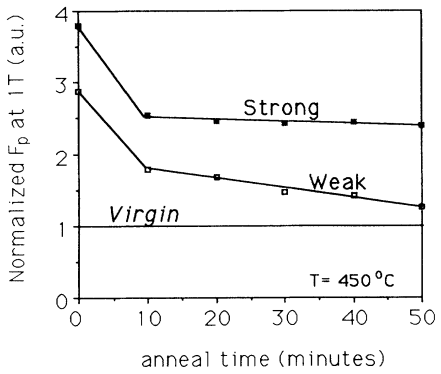

FIG. 5. Isothermal recovery at 450 °C: normalized F_p (to the virgin state) at 1 T, for strong (S3) and weak (S4) native pinning samples, characterized at 10 K.

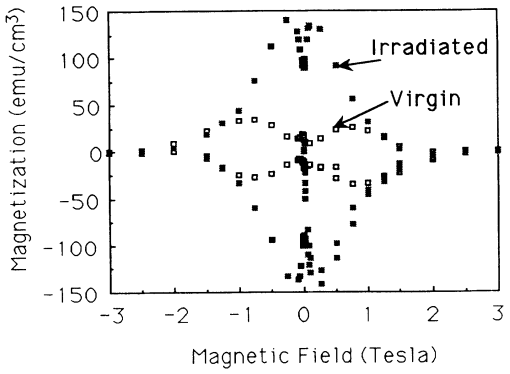

FIG. 6. Magnetic hysteresis loops for sample 3, a strong native pinner, before and after irradiation, characterized at 77 K.

than at 10 K, most likely because of the difference in the flux lattice, rigid vs liquidlike, at these two temperatures. However, sample 4, a weak-pinning sample at 77 K in the virgin state, receives no indicative enhancement of the properties after irradiation. Because there is no enhancement, the sample will not be used for the isothermal recovery analysis at 77 K.

2. *Annealing experiments*

For the annealing study, the raw data were converted to a normalized area ($A_{T\ \mathrm{anneal}}/A_{\mathrm{virgin}}$), where the area corresponds to $(\delta M)B$ or $\sim F_p(\ln B)$: a "magnetization energy" product. This was done in consideration of the nonphysical loops (Fig. 6) that are obtained from the magnetometer where there is a pronounced dip at 0 T in the data. We do not understand these loops, but find them to be reproducible. It must be noted that similar loops have been reported by other groups.[7] The minimum in the magnetization loops makes the "apparent" J_c and F_p values very sensitive to the magnetic field. In order to analyze the data, we chose to calculate the area of the loop, which is as valid as calculating F_p because the area is proportional to the flux-pinning force. Furthermore, by calculating the area, any error in a stray data point would be minimized.

Figure 7 reveals similar annealing results as the 10-K isochronal data. Between 100 and 450 °C, there is little change in the flux-pinning force or energy, but after 450 °C, both samples approach the virgin state. The strong-pinning sample (S2) holds onto the added enhancement until 600 °C, whereas the weak-pinning sample (S1) drops off at 500 °C and then remains constant. These annealing effects follow the same conclusion as the 10-K data.

There is a difference in the 77-K data for the first annealing temperature of 100 °C. Both samples show a considerable drop-off in flux-pinning energy: Both achieve about 50% recovery and even more for the weak-pinning sample. It was verified that the significant drop in pin-

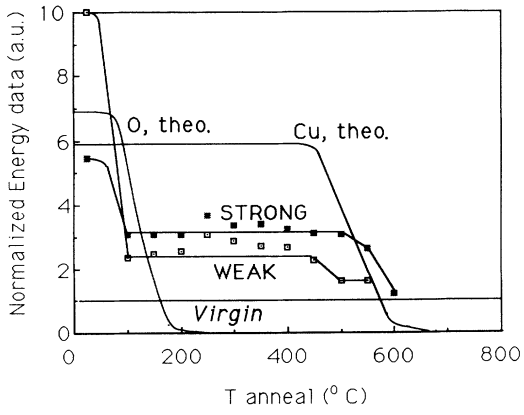

FIG. 7. Isochronal recovery at 77 K: normalized magnetization energy vs annealing temperature for strong (S2) and weak (S1) native pinning samples with superimposed theoretical annealing curves for Cu and O point defects.

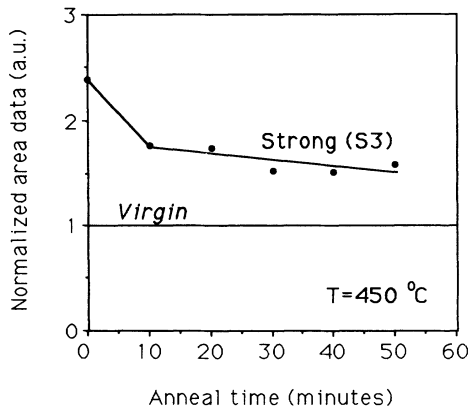

FIG. 8. Isothermal recovery at 77 K: experimental normalized magnetization energy vs annealing time for a strong (S3) native pinning sample.

ning was not due to time relaxation between irradiation and first anneal characterizations. Time was allowed after irradiation before characterization to minimize these effects, and a period of 3 months passed before the annealing study began. One sample was recharacterized before the first anneal to compare the irradiation hysteresis loops and the time-delayed preanneal loops. No difference was found. Because of the difference in the two apparent recovery temperatures, 100 and 450 °C, this indicates two stages of relaxation. Note, also, that the 77-K data do not achieve full recovery to the virgin state as did the 10-K data.

For the isothermal anneals at 450 °C, similar annealing effects (Fig. 8) occur as in the 10-K data. Furthermore, these data provide more evidence for two stages of recovery.

IV. THEORY

For high-energy proton radiation, there are two types of radiation-induced pins possible. The most difficult to study by conventional methods are atomic point defects produced by proton and ion knock-ons. These are ion vacancy and interstitial pairs, the displacements that TRIM calculates. Recovery for these defects takes place by recombination through short-range lattice diffusion. Note that for all Frenkel pairs produced during irradiation, room-temperature annealing occurs simultaneously; therefore, only the uncorrelated pairs would still exist. However, the amount of room-temperature annealing is approximated to be around 13%,[8] which would not affect our results dramatically.

The other type of flux pinners that could exist are defect clusters: agglomerates of point defects. Relaxation of defect clusters would occur by diffusional processes through long-range lattice diffusion. If dissolution of clusters is responsible for the relaxation of excess pinning, we can use the relaxation temperatures (100 and 450 °C), combined with the diffusivity of O, Cu, Ba, and Y at these temperatures, to infer the effective diffusion range:

$$X_{\text{eff}}=\sqrt{D(T)t} \ .$$

If we assume that the clusters involve a substantial number of the proton-irradiated-induced defects, we can also infer their size.

To distinguish the defects responsible for the enhanced pinning, recovery equations can model the type and species. The general equation for the defect concentration is[9]

$$\frac{dC_i}{dt}=K-\alpha C_i C_v-k_i^2 D_i C_i \ ,$$

where K is the defect production rate, α is the recombination coefficient, and k_i^2 is a term that includes the loss of point defects to different types of sinks (e.g., grain boundaries, loops, cracks, etc.). The equation for α is

$$\alpha=\frac{4\pi r_{iv}}{V_a}D \ ,$$

where r_{iv} is the closest distance between defect and sink before recovery occurs, D is the diffusivity of the species, and V_a is the atomic volume of the material.

For point-defect annihilation, the rate equation becomes

$$\frac{dC_i}{dt}=-\alpha C_i^2 \ ,$$

and this is integrated to obtain the recovery equation

$$C_i(t)=C_v(t)=\frac{C_0}{1+\alpha C_0 t} \ ,$$

where C_0 is the fractional concentration of defects.

Table IV summarizes the values and diffusivities used to obtain the theoretical recovery curves for point-defect annihilation. The diffusivities were extrapolated from the data of Rothman, Routbort, and Welp,[10] and Chen.[11] The results for a 10-min isochronal recovery are shown in Fig. 9. No curve was calculated for yttrium because of the insufficient diffusional data.

Recovery occurs over very narrow temperature ranges, about 100 °C, and so we can define recovery temperatures for each of the ions. As is expected, recovery proceeds according to the diffusivity: from light, fast ions (oxygen at 100 °C) to slow, large species (Cu at 470 °C and Ba at 770 °C). The largest ion, yttrium, would have a recovery temperature above 770 °C, since its diffusivity is smaller than Ba.[11]

For the isothermal anneals, with $T=450$ °C, theoreti-

TABLE IV. Variables and values or equations utilized in the theoretical recovery equation.

Variable	Value or equation
r_{iv}	$a_0, 3a_0$
V_a	13 Å/atom
D_{O}	$1.5[(1.4e-4)\exp(-93.61\ \text{kJ/8.314 T})]$
D_{Cu}	$7.3\exp(-260\ \text{kJ/8.314 T})$
D_{Ba}	$6.94e26\exp(-890\ \text{kJ/8.314 T})$

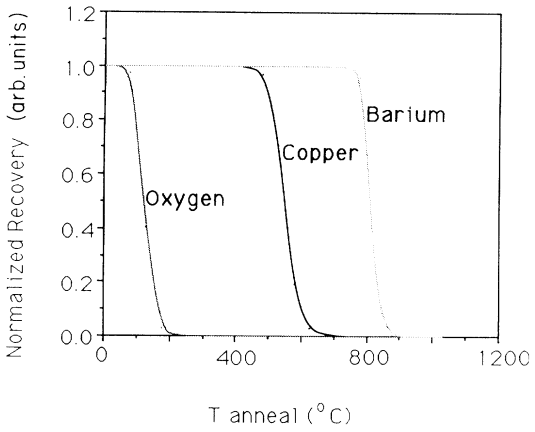

FIG. 9. Theoretical isochronal recovery curves: point-defect concentration (normalized to prerecovery state) vs annealing temperature.

cal oxygen and copper recovery versus time curves are illustrated in Fig. 10. For the oxygen ions, rapid annihilation is predicted and verified by the concentration drop-off in the first 3 min. At 450 °C—the edge of the recovery curve for copper point-defect annihilation—we should see no recovery proceeding as the horizontal line illustrates. Time-dependent copper-defect recovery at an elevated temperature is included in this figure to correspond to a higher diffusivity. The diffusional equation used for the copper recovery curve was obtained from high-temperature data, and the possibility of a small difference in the diffusivity at 450 °C can be expected.

V. DISCUSSION

Figures 4 and 7 show the 10-K, 77-K, and the normalized theoretical isochronal recovery curves together. Note the correlation between the copper recovery temperature and the actual recovery data. This indicates that copper point defects are potent radiation-induced flux pinners. Also, they exist as enhancing pinners up to

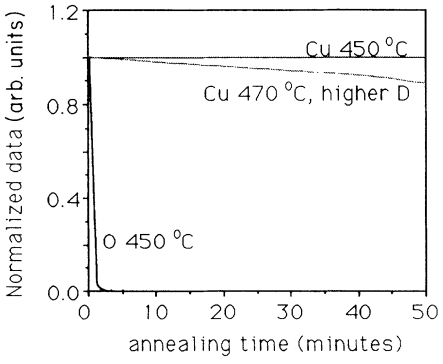

FIG. 10. Theoretical isothermal recovery curves: point-defect concentration (normalized to preanneal) vs time for copper and oxygen.

450 °C. The data at 77 K, where the flux lattice is not rigid, shows another flux pinner annihilating at 100 °C, which corresponds to the oxygen point-defect recovery curve. Furthermore, the strong-pinning native sample seems to indicate oxygen point defects also when characterized at 10 K.

For the isothermal anneals, both characterization temperatures reveal two types of enhancing flux pinners. The substantial recovery in the first 10 min against the gradual recovery between 20 and 50 min indicates two flux-pinning species annealing away. Figure 10 postulates that oxygen point defects are annihilating in the first 10 min and then the copper point defects are annealing slowly in the first 50 min. The fact that some samples show gradual annihilation and another sample does not could be an indication that the actual Cu diffusivity is slightly higher than expected or the samples were annealed at a slightly higher temperature than 450 °C in the box furnace. For the theoretical recovery curves, 450 °C is the shoulder temperature before annealing occurs; however, experimentally, three samples reveal gradual annealing. This does not mean that copper defects are not the enhanced pinners, just that there is probably a difference between extrapolated diffusivity data and the actual copper diffusivity at 450 °C.

The experimental data correlate with the model of oxygen and copper point defects from their theoretical curves. The coherence length ξ_{ab} in the YBCO material is around 1.5 nm.[12] Therefore any defects on the order of the coherence length would be effective as pinning sites.[13] This is consistent with a point defect. If we assume that a single Cu vacancy on the Cu-O planes depresses the superconductivity to its nearest neighbors, the size of the depression zone is about twice the Cu-Cu spacing or 0.776 nm. This is similar to ξ_{ab}. With the expected density of point defects and the needed coherence length size for enhanced pinning, the result of copper and oxygen point defects producing the enhanced pinning after irradiation matches with the model of many point defects inhibiting the motion of a vortex. Barium and yttrium Frenkel pairs must not play a role in the excess pinning because the critical current density J_c recovers at annealing temperatures well below the Ba and Y point-defect recovery temperatures.

Now even though the data justify point defects as the radiation-induced flux pinners, there are observations of 30-Å-size defect clusters, in low density, produced by proton irradiation of YBCO single crystals.[14] They calculate the defect concentration of these clusters to be 65 ppm or about 10% of the radiation-induced defects end up as visible defects in the transmission electron microscope (TEM). The fact that there is a low density of these defects cannot make them the only defects responsible for the large enhancement of the superconducting properties; however, their size is equal to $2\xi_{ab}$, which is of the order for efficient flux pinning. But the nature—type and species—of these clusters has not been revealed. Looking at the curves for the isothermal anneals (Figs. 5 and 8), we observe two species annealing at 450 °C for 50 min. The theoretical curves infer oxygen point defects as the rapid annealing species; however, since oxygen is a fast

diffuser, we must investigate the possibility of oxygen clusters as an alternative rapid annealing type. The effective diffusion distance for the clusters would be governed by the equation $X_{\text{eff}}=\sqrt{D(T)t}$, and at 450 °C for 10 min, the value would be 1.78 μm. Thus, for vacancies and interstitials to annihilate, they must cover a distance of 1.78 μm. For clusters to exist after irradiation, their separation distance of 1.78 μm corresponds to a cluster density of about $10^{11}/\text{cm}^3$. Assuming that 13% of the oxygen defects do relax during irradiation, the expected density of these defects is about $10^{17}/\text{cm}^3$, and so the number of defects per cluster would be 10^6. With each defect taking up an average of 4 Å of space, this means that the diameter of each cluster would be around 200 Å, much larger than what is seen in the TEM. Therefore it is unlikely that oxygen clusters are responsible for the great enhancement of the superconducting properties, and this provides more evidence that oxygen point defects are the fast annealing species revealed in the experimental isothermal curves.

We must consider the possibility of point defects and clusters coexisting, especially with defect clusters of mixed species. The theoretical analysis of this combination is beyond the scope of this paper. However, as stated in preceding paragraphs, the TRIM calculations with the theoretical and actual recovery curves provide evidence to support large densities of defects. And with this many copper and oxygen defects coexisting in the crystal, it is of great probability that there are spatially correlated (nearby) defects of unlike species. These point defects would result in the enhancement of the superconducting properties by producing a larger area of superconductivity suppression while still annealing out at their specific recovery temperature.

Considering the thickness of the crystals, they are not radiation transparent—hydrogen ions are implanted into the crystal. Both sides of the crystals are irradiated for maximum effect to the superconducting properties, but either one or two dead zones are produced, depending on the crystal's thickness (see Table III). A dead zone corresponds to a high-dose irradiation from end-of-range effects, resulting in a nonsuperconducting area. The magnitude of the enhancement of the crystal properties correlates with groups who used transparent crystals,[14] and so the dead zones do not affect the pinning enhancements we observe. Also, the critical temperature does not change after irradiation or annealing; therefore, the hydrogen is not playing an effect in the recovery. These thin slices of nonsuperconducting material are not the radiation-induced pinners since for anneals up to 600 °C ($T_{\text{char}}=10$ K), all crystals achieve full recovery to the virgin state.

VI. CONCLUSIONS

In summary, this study has verified that irradiation of YBCO single crystals with 3.4-MeV protons to a dose of $10^{16}/\text{cm}^2$ increases the superconducting properties (J_c, F_p) dramatically without degrading the critical temperature. By performing isochronal and isothermal annealing experiments, we have seen the recovery of the enhanced flux pinning to or near the virgin state (preirradiated) by 600 °C. Relaxation occurs in two stages: one enhancement recovery stage by 100 °C and a second stage at 450 °C.

Theoretical Frenkel-pair annihilation curves were calculated from the Ullmaier-Schilling model[9] using the data of Rothman, Routbort, and Welp.[10] The results conclude that oxygen Frenkel pairs recombine between 100 and 200 °C, copper Frenkel pairs between 450 and 600 °C, and barium Frenkel pairs between 800 and 900 °C. Slowly diffusing yttrium was not considered. And it was determined that oxygen clusters would anneal away at a higher temperature than 450 °C.

Since the model of point defects is coincident with the observed annealing range and pattern of recovery (more than one species), we conclude that oxygen and copper point defects are responsible for the excess pinning. The model of the copper and oxygen point defects as the flux pinners has great merit because of the apparent density of these defects and a favorable size correlation to the coherence length for maximum pinning efficiency. Moreover, since superconductivity in the YBCO system is linked to the copper-oxygen planes and chains, it would seem likely that the enhanced pinning would be a consequence of producing defects of these species.

ACKNOWLEDGMENTS

We would like to thank Dr. Gary Was and co-workers for the use of the accelerator and informative discussions. Thanks must also be given to Frank Parker who maintains the SQUID magnetometer, to Dr. B. J. Evans and his research group for the use of their box furnace, and to T. A. Vanderah for supplying the single crystals.

[1] W. K. Chu, J. R. Liu, and Z. H. Zhang, Nucl. Instrum. Methods B **59-60**, 1447 (1991).

[2] J. W. Lee, H. S. Lessure, D. E. Laughlin, M. E. McHenry, S. G. Sankar, J. O. Willis, J. R. Cost, and M. P. Maley, Appl. Phys. Lett. **57**, 2150 (1990).

[3] R. B. van Dover, E. M. Gyorgy, A. E. White, L. F. Schneemeyer, R. J. Felder, and J. v. Waszczak, Appl. Phys. Lett. **56**, 2681 (1990).

[4] T. A. Vanderah, C. K. Lowe-Ma, D. E. Bliss, M. W. Decker, M. S. Osofsky, E. F. Skelton, and M. M. Miller, J. Cryst. Growth **118**, 385 (1992).

[5] J. F. Ziegler, J. P. Biersack, and U. Littmark, *The Stopping and Range of Ions in Solids* (Pergamon, New York, 1984), version TRIM'91.

[6] M. Griffith, Master's thesis, The University of Michigan, 1992.

[7] P. Fischer, R. Busch, H. W. Neumuller, G. Ries, and H. F. Braun, Supercond. Sci. Technol. **5**, S1 (1992), pp. 5440–5443.

[8] V. Naundorf, J. Nucl. Mater. **182**, 254 (1991).

[9] H. Ullmaier and W. Schilling, *Physics of Modern Materials* (Vienna International Atomic Energy Agency, Vienna, 1980), p. 30.

[10] S. J. Rothman, J. L. Routbort, and U. Welp, Phys. Rev. B **44**,

2326 (1991).
[11]Nan Chen, Ph.D. thesis, Illinois Institute of Technology, 1991.
[12]P. H. Kes, in *Phenomenology and Applications of High Temperature Superconductors* edited by K. S. Bedell (Addison-Wesley, New York, 1992).
[13]T. Matsushita, Cryogenics **30**, 817 (1990).
[14]L. Civale, M. W. McElfresh, A. D. Marwick, T. K. Worthington, A. P. Malozemoff, F. Holtzberg, C. Feild, J. R. Thompson, D. K. Christen, and M. A. Kirk, in Proceedings of the XII Winter Meeting on Low Temperature Physics, 1991 (World Scientific, Singapore, in press).

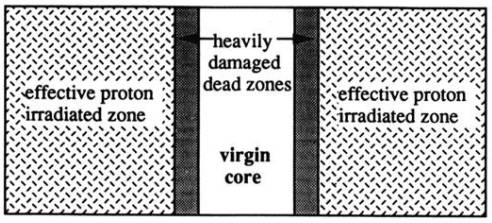

FIG. 2. Spatial irradiation regions in a single crystal of YBCO which is not proton transparent in thickness.